Journal of Inflammation Research

Dovepress
open access to scientific and medical research

Open Access Full Text Article

ORIGINAL RESEARCH

# PANoptosis and Autophagy-Related Molecular Signature and Immune Landscape in Ulcerative Colitis: Integrated Analysis and Experimental Validation

Jiali Lu[1,2,*], Fei Li[3,*], Mei Ye[1,2]

[1]Department of Gastroenterology, Zhongnan Hospital, Wuhan University, Wuhan, Hubei, 430071, People's Republic of China; [2]Hubei Clinical Center and Key Laboratory of Intestinal and Colorectal Diseases, Zhongnan Hospital, Wuhan University, Wuhan, Hubei, 430071, People's Republic of China; [3]Center for Evidence-Based and Translational Medicine, Zhongnan Hospital of Wuhan University, Wuhan, Hubei, 430071, People's Republic of China

*These authors contributed equally to this work

Correspondence: Mei Ye, Department of Gastroenterology, Zhongnan Hospital, Wuhan University, Wuhan, Hubei, 430071, People's Republic of China, Email wumeiye08@163.com



**Background:** Ulcerative colitis (UC) is an autoimmune inflammatory disorder of the gastrointestinal tract. Programmed cell death (PCD), including PANoptosis and autophagy, plays roles in inflammation and immunity. This study aimed to investigate the molecular signature and immune landscape of the PANoptosis- and autophagy-related differentially expressed genes (DEGs) in UC.

**Methods:** Analyzing UC dataset GSE206285 yielded DEGs. Differentially expressed PANoptosis- and autophagy-related genes were identified using DEGs and relevant gene collections. Functional and pathway enrichment analyses were conducted. A protein-protein interaction (PPI) network was established to identify hub genes. TRRUST database predicted transcription factors (TFs), pivotal miRNAs, and drugs interacting with hub genes. Immune infiltration analysis, UC-associated single-cell sequencing data analysis, and construction of a competing endogenous RNA (ceRNA) network for hub genes were conducted. Machine learning identified key candidate genes, evaluated for diagnostic value via receiver operating characteristic (ROC) curves. A UC mice model verified expression of key candidate genes.

**Results:** Identifying ten PANoptosis-related hub DEGs and four autophagy-related hub DEGs associated them with cell chemotaxis, wound healing and positive MAPK cascade regulation. Immune infiltration analysis revealed increased immunocyte infiltration in UC patients, with hub genes closely linked to various immune cell infiltrations. Machine learning identified five key candidate genes, TIMP1, TIMP2, TIMP3, IL6, and CCL2, with strong diagnostic performance. At the single-cell level, these genes exhibited high expression in inflammatory fibroblasts (IAFs). They showed significant expression differences in the colon mucosa of both UC patients and UC mice model.

**Conclusion:** This study identified and validated novel molecular signatures associated with PANoptosis and autophagy in UC, potentially influencing immune dysregulation and wound healing, thus opening avenues for future research and therapeutic interventions.

**Keywords:** ulcerative colitis, PANoptosis, autophagy, immune cell infiltration, inflammatory fibroblasts, bioinformatics analysis

## Introduction

Ulcerative colitis (UC), an inflammatory bowel disease (IBD) characterized by relapsing, incurable, chronic inflammation of the colon, with a prevalence exceeding 400 per 100,000 in North America.[1] Patients with persistent UC suffer poor quality of life accompanied by chronic diarrhea, rectal bleeding, and a higher risk for developing colitis-associated colorectal cancer (CAC).[2] Although the exact etiology of UC remains currently obscure, factors such as genetic susceptibility, dysregulated barrier and mucosal immune homeostasis, and environmental influences, including gut microbiota, have been implicated in its pathogenesis.[3,4] It is widely acknowledged that a vicious cycle of dysregulated cell death, compromised intestinal barrier, and

Received: 20 December 2023
Accepted: 16 May 2024
Published: 20 May 2024

subsequent aberrant immune inflammatory response rests at the core of chronic inflammatory gastrointestinal conditions.[5] Various cell death processes, like necroptosis, pyroptosis, ferroptosis and autophagy are important modes of programmed cell death (PCD) in the intestine in addition to apoptosis. The research on intestinal cell death programs may contribute to understanding the biology and pathogenesis of UC and is expected to be an important strategy for its prevention and treatment; further investigation is required.

PANoptosis, a newly recognized pathway for proinflammatory PCD, highlights the crosstalk and coordination of pyroptosis, apoptosis, and necroptosis.[6,7] This unique inflammatory PCD modality is regulated by multifaceted PANoptosome complexes that are assembled by key components that perform other PCD pathways.[8,9] PANoptosis has been associated with infectious, neurodegenerative, autoinflammatory, metabolic diseases, and cancer.[10,11] Given the important roles of pyroptosis, apoptosis, and necroptosis in IBD,[12–14] we may speculate that PANoptosis and the occurrence of UC are closely connected. However, limited studies have explored the role of PANoptosis in UC pathogenesis.

Autophagy, a cellular catabolic process, exhibits strong connections with intestinal biology and function. It serves as a primary mechanism for restoring homeostasis and repairing intestinal damage under low-level stimuli or pathogen infections, whereas autophagic capacity is overwhelmed, it is likely to trigger apoptosis.[4,15] It was also reported that the crosstalk between autophagy and inflammasome activation, compromised autophagy induced the aberrant inflammasome activation.[16] Dysfunctional autophagy may lead to disrupted intestinal homeostasis, gut dysbiosis, aberrant immune responses and amplifying intestinal inflammation, which are strongly connected with IBD progression.[17] Genome-Wide Association Studies (GWAS) and subsequently functional research have revealed numerous autophagy genes participate in IBD pathology.[18–20] Moreover, autophagy-related gene, ATG4B-deficient mice were more susceptibility to dextran sodium sulfate (DSS)-induced colon colitis.[21]

In this study, we aimed to identify the differentially expressed PANoptosis- and autophagy-related hub genes in UC using bioinformatics analysis. We investigated the correlations between these hub genes and circulating immune infiltration as well as their expression levels at the single-cell level. Furthermore, by performing machine learning algorithms and validating in colon mucosa of UC patients and UC mice model, we identified five key candidate genes that may serve as the potential biomarkers and therapeutic targets for UC progression. Our findings may contribute to take efforts to develop UC diagnosis and treatments based on modulating PANoptosis and autophagy.

# Materials and Methods

## Data Sources

We initiated our study by using the keyword “ulcerative colitis” to search for appropriate datasets in the Gene Expression Omnibus (GEO) database (http://www.ncbi.nlm.nih.gov/geo/). Finally, we included seven datasets on intestinal mucosal expression from UC patients, including GSE206285, GSE87466, GSE16879, GSE75214, GSE114527, GSE73661, and GSE92415.[22–28] The information corresponding to all datasets in the study was shown in Table 1. The list of 274 PANoptosis-related genes (PRGs) was obtained from previous research which combined with the apoptosis, pyroptosis and necroptosis gene sets.[29] 794 autophagy-related genes (ARGs) were obtained from the Autophagy Database (HAMdb),[30] (Supplementary Table 1).

**Table 1** The Information Corresponding to All Datasets in the Study

| Datasets | Platform | Tissues | UC Samples | Control Samples |
|---|---|---|---|---|
| GSE206285 | GPL13158 | Colon mucosa | 550 | 18 |
| GSE87466 | GPL13158 | Colon mucosa | 87 | 21 |
| GSE16879 | GPL570 | Colon mucosa | 48 | 6 |
| GSE75214 | GPL6244 | Colon mucosa | 97 | 11 |
| GSE114527 | GPL14951 | Rectal mucosa | 32 | 6 |
| GSE73661 | GPL6244 | Colon mucosa | 166 | 12 |
| GSE92415 | GPL13158 | Colon mucosa | 162 | 21 |
| SCP259 | 10X GemCode or Chromium | Colon mucosa | 18 | 12 |

## Differential Expression Analysis

To identify genes associated with UC pathogenesis, we used the "limma" package (version 3.54.0) in R software (version 4.3.1) to investigate DEGs in GSE206285 dataset, and the threshold value was set at $|\log_2$ (Fold Change) $| > 1$ and adjusted $p$-value $< 0.05$. The crossover genes between DEGs and PRGs were referred to differentially expressed PANoptosis-related genes (DE-PRGs), as assessed by the "UpSetR" package (version 1.4.0). Genes that crossed over between DEGs and ARGs were referred to differentially expressed autophagy-related genes (DE-ARGs), as assessed by the "VennDiagram" R package (version 1.7.3).

## Functional Enrichment Analysis

Subsequently, we performed Gene Ontology (GO) and Kyoto Encyclopedia of Genes and Genomes (KEGG) annotation to analyze the biological functions of the identified DEGs, DE-PRGs and DE-ARGs utilizing "clusterProfiler" R package (version 4.8.2), with adjusted $p$-value $< 0.05$ considered as statistically significant. In addition, the Metascape database[31] was used to further conduct pathway enrichment and bioprocess annotation.

## Construction of Protein-Protein Interaction (PPI) Network and Identification of the Hub Genes

To unravel the intricate network of interactions among DE-PRGs and DE-ARGs, we constructed PPI networks using the STRING database.[32] The PPI network was visualized using Cytoscape software (version 3.10.0), and utilizing Cytoscape plug-in (MCODE and MCC), we identified the hub genes crucial in the context of PANoptosis and autophagy. Subsequent functional enrichment analyses were also conducted to gain insights into the biological roles of these hub genes using the "clusterProfiler" R package (version 4.8.2) and the Metascape database.

## The Hub Genes and Their Interactions

Expanding our analysis, we explored the regulatory landscape surrounding the identified hub genes. We introduce the hub genes into TRRUST database[33] and obtained interactional transcription factors (TFs). Differential expression of these TFs in the training dataset GSE206285 was analyzed using the "limma" R package. Utilizing miRTarBase database,[34] we obtained corresponding interacted miRNA to each hub gene. In addition, the hub gene-drug interactions were mined using DrugBank database.[35] The above interactive networks were visualized by Cytoscape software (version 3.10.0).

## Immune Infiltration Analysis

Understanding the immune microenvironment in UC is crucial. We used the "CIBERSORT" R package[36] to analyze immune cell infiltration landscape of UC patients and normal groups in GSE206285 dataset. Pearson's correlation analysis was conducted to test the relationships between the hub gene expression profiles and immune cells, and used the "corrplot" software package (version 0.92) to visualize their correlation heatmaps. $P$ value $< 0.05$ is considered statistically significant.

## Single-Cell Sequencing Data Analysis

To further analyze the cellular distribution and expression of the hub genes in different cell subsets within the colon mucosa, we searched the Single Cell Portal website (https://singlecell.broadinstitute.org/) for datasets related to "ulcerative colitis", and screened UC-associated single-cell sequencing data (SCP259),[37] which identified 51 cell subsets in colon mucosa of 18 UC and 12 healthy individuals. Uploading a list of the hub genes and exploring the expression of the hub genes from epithelial, immune and stromal clustering with the annotation of cluster and health, respectively. Visualized by dot plot.

## Construction of the lncRNA–miRNA–mRNA ceRNA Network

To uncover additional layers of gene regulation, we constructed competing endogenous RNA (ceRNA) networks involving hub genes, miRNAs, and lncRNAs. First, we mined miRNAs associated with the hub genes from the three databases of

miRTarBase,[34] DIANA-TarBase v8[38] and TargetScan,[39] and intersected. Then, the obtained overlapping miRNAs were introduced into the starBase database[40] for predicting of miRNA-lncRNA interactions. The collected lncRNAs-miRNAs-hub genes regulatory networks were visualized by Cytoscape software (version 3.10.0).

## Construction of the Diagnostic Model and Identification of the Key Candidate Genes

In our pursuit of clinical translation, we employed least absolute shrinkage and selection operator (LASSO) regression analysis using the "glmnet" R package (version 4.1–8) to construct the diagnostic model and identify key candidate genes related to UC diagnosis. LASSO regression is a machine learning technique that combines variable selection and regularization to increase prediction accuracy,[41] and displaying the relationship between the identified key candidate genes by using the "circlize" R package (version 0.4.15). We further assessed the diagnostic efficacy of the key candidate genes by Receiver Operating Characteristic Curve (ROC) analysis performed by using "pROC" software package (version 1.18.4). The area under the ROC curve (AUC) was obtained and genes with AUC value > 0.7 were regarded as benefit for disease diagnosis.

## Animal Experiments

Additionally, we validated key candidate genes identified through our analyses using UC mice model. C57BL/6 wild type (WT) mice were obtained from the Institute of Model Animals, Wuhan University. All mice were raised under specific pathogen-free conditions, undergoing a one-week acclimatization period before the start of the experiments. To induce acute colitis, four male mice were fed with 2.5% DSS (MP Biomedicals) in their drinking water for 5 days, and they were assigned to the experimental group. The other four male mice were fed with regular water throughout and assigned to the control group. After the conclusion of the experiment, mice were euthanized by cervical dislocation following intraperitoneal injection of sodium pentobarbital anesthesia, and the entire colon tissue was collected. Approximately 1 cm of colon tissue from the distal rectum was prepared as paraffin sections and subjected to H&E staining. Another suitable segment of colon tissue was extracted to obtain total RNA for quantitative real time PCR (qRT-PCR) analysis. All animal experimental procedures were approved by the Animal Ethics committee of Zhongnan Hospital, Wuhan University.

## Specimen Collection

Colonic mucosal tissues from 12 patients with active UC and 12 age- and sex-matched healthy volunteers were collected during endoscopic procedure from Zhongnan Hospital of Wuhan University (Wuhan, China). All patients with UC were diagnosed based on clinical standard, endoscopic features, and original histopathological detection, confirming the active inflammatory status of the patients. None of the patients received immunosuppressants, steroids, or biologics treatment. The study was approved by the Medical Ethics Committee, Zhongnan Hospital of Wuhan University (Scientific Ethical Approval No.2022011K).

## RNA Extraction and qRT-PCR Analysis

Finally, we validated the expression of key candidate genes through qRT-PCR. Total RNA from colonic mucosal tissues was extracted using TRIzol reagent (Invitrogen, USA) and the TOYOBO ReverTra Ace kit (TOYOBO, Japan) was used for cDNA synthesis according to the manufacturer's protocols. Then, qRT-PCR was conducted using UltraSYBR Mixture (CWBIO, China) on a LightCycler96 (Roche, USA). We used the $2^{-\Delta\Delta Ct}$ quantification method to determine the expression levels of key candidate genes, with GAPDH serving as an endogenous control. The primers were designed using the Primer Bank website[42] and all primer sequences are listed in Supplementary Table 2.

## Statistical Analysis

The experimental data are presented as the mean ± SEM. The two groups were compared using an independent Student's *t*-test based on statistically significant differences in normally distributed variables. For non-normally distributed variables, analysis was performed using the Mann–Whitney *U*-test (Wilcoxon rank-sum test). One-way ANOVA was used for more than two comparison groups. Statistical analyses were performed with GraphPad Prism 9.0.0 (GraphPad

Software, USA) for comparison. Descriptive statistics of the clinical information were analyzed using statistical software SPSS (v 25.0). Normally distributed continuous data were presented as mean ± SEM, while non-normally distributed data were presented as median and interquartile range (IQR). P values less than 0.05 indicated statistical significance.

# Results

## Differential Expression Analysis

We first analyzed the integrated UC dataset GSE206285, identifying a total of 2490 DEGs, including 1380 upregulated genes and 1110 downregulated genes using the "limma" R package (Figures 1A and B). Subsequently, we conducted GO analysis to categorize the DEGs and performed KEGG pathway enrichment analysis on the 2490 DEGs to explore their potential role (Supplementary Figure 1). Next, we identified 71 PANoptosis-related DEGs, encompassing 46 apoptosis genes, 14 necroptosis genes, and 11 pyroptosis genes, employing an upset diagram. Additionally, we obtained 113 autophagy-related DEGs using a venn diagram (Figures 1C and D, Supplementary Box 1).

## Functional and Pathway Enrichment Analysis

To delve deeper into the functional roles of PANoptosis- and autophagy-related DEGs, we performed GO analysis and KEGG pathway enrichment analysis. The PANoptosis-related DEGs were mainly enriched in the biological process (BP)

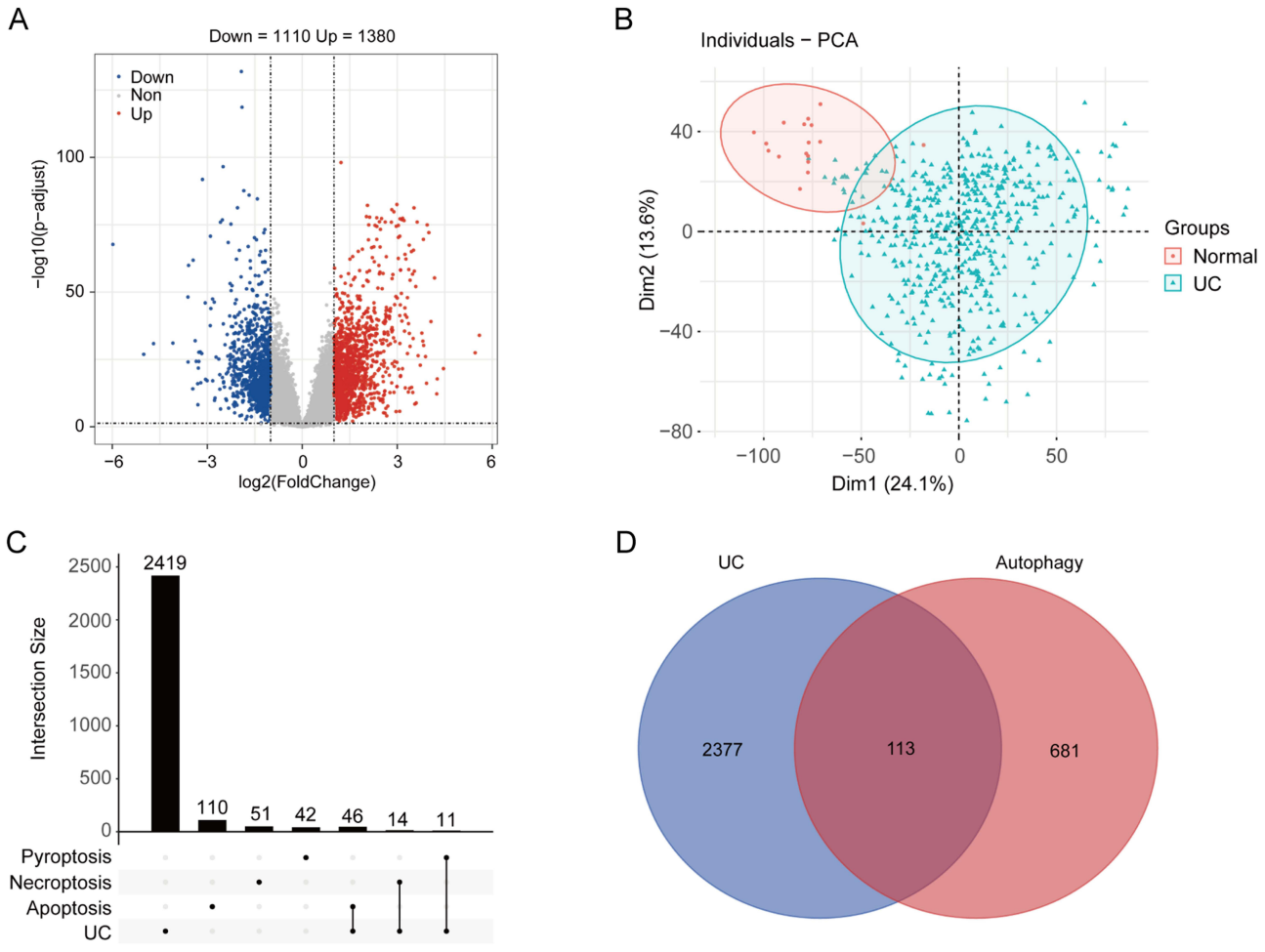


**Figure 1** Identification of DEGs in the UC dataset. (**A**) Volcano map of the DEGs in UC patients versus the healthy subjects in GSE206285. Blue dots represent downregulated genes, red dots represent upregulated genes and grey dots show genes with no significant difference with a threshold of |log2FC| >1 and adjusted to $p < 0.05$. (**B**) PCA showed the gene cluster between UC and healthy subjects. (**C**) An Upset diagram of UC-related DEGs as well as pyroptosis, necroptosis and apoptosis. (**D**) A Venn diagram of the intersection of UC-related DEGs and autophagy-related genes.

of wound healing, regulation of peptidase activity and positive regulation of cytokine production, and were closely related to the cellular component (CC) of the collagen-containing extracellular matrix. In the molecular function (MF) categories, protease binding and peptidase regulator activity were discovered (Figure 2A). Besides, KEGG enrichment analysis demonstrated their involvement in pathways associated with cancer, infections, TNF signaling pathway and NF-κB signaling pathway (Figures 2B). Furthermore, according to Metascape enrichment analysis, these PANoptosis-related DEGs were enriched in pathways such as positive regulation of programmed cell death, response to wounding, cytokine signaling in Immune system and cellular response to cytokine stimulus (Figures 2C).

Similarly, the autophagy-related DEGs displayed enrichment in regulation of autophagy, regulation of angiogenesis and response to molecule of bacterial origin (Figure 3A). The KEGG pathway enrichment analysis demonstrated enrichment of PI3K-Akt signaling pathway, Proteoglycans in cancer, and mTOR signaling pathway (Figure 3B). Furthermore, we utilized an alternative visualization method, confirming that the enriched pathways were consistent with the results of GO analysis (Figures 3C).

## Identification of the Hub Genes

Further analysis led to the identification of the hub genes within the PANoptosis and autophagy networks. As illustrated in the PPI network of PANoptosis-related DEGs, we found 10 overlapping hub genes (PDGFRB, TIMP1, MMP2, CD44, TIMP2, TGFB2, IL6, TIMP3, IL1B, HGF) using the Cytoscape plug-in (MCODE and MCC) (Figures 4A-C). Similarly, in the PPI network of autophagy-related DEGs, CCL2, TGFB1, PPARG and CXCR4 were identified as the hub genes (Figures 4D-F).

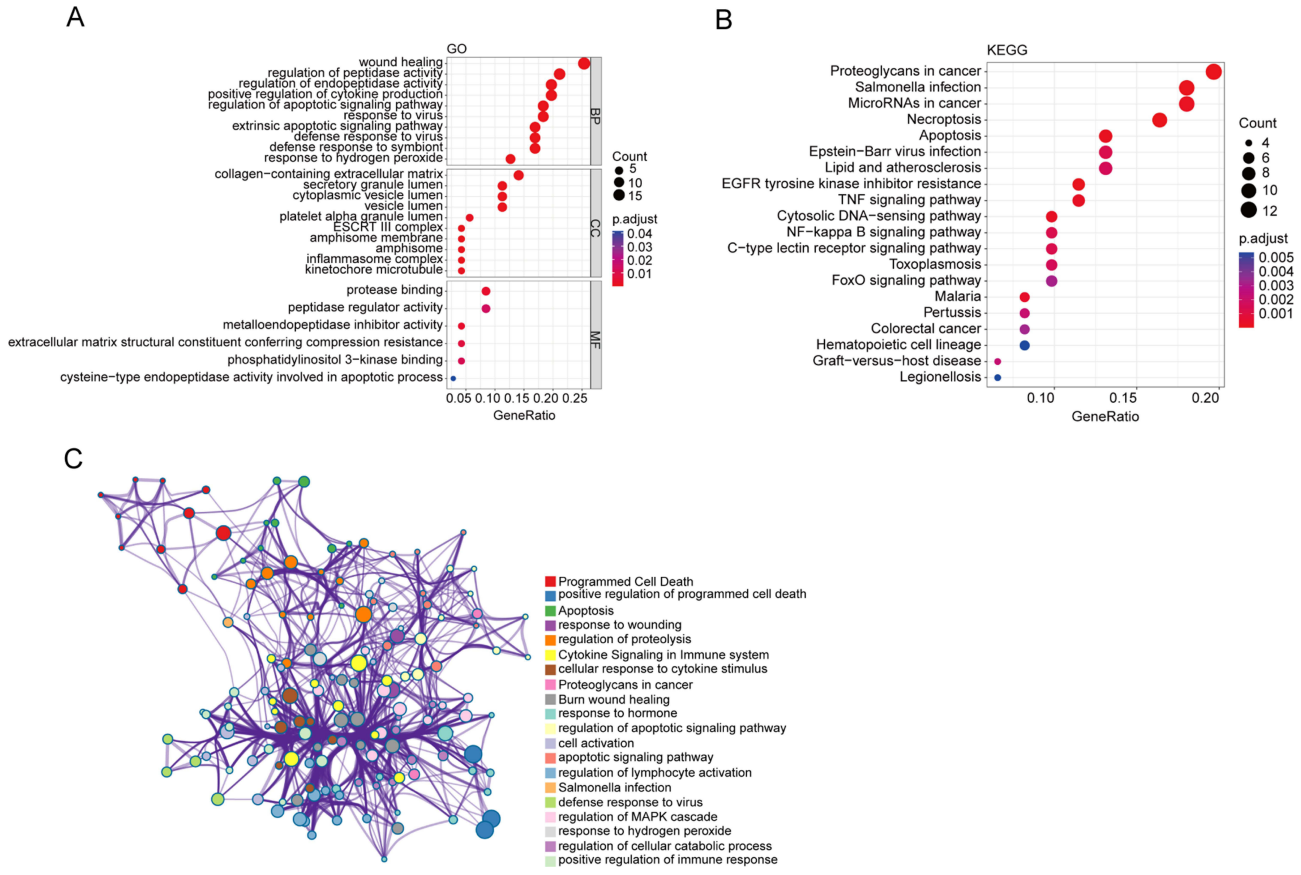


**Figure 2** Functional annotation of the PANoptosis-related DEGs. (**A**) GO enrichment analysis of the PANoptosis-related DEGs using R software. (**B**) KEGG enrichment analysis of the PANoptosis-related DEGs using R software. (**C**) The pathways network of the PANoptosis-related DEGs showing the intra-cluster and inter-cluster connections of enriched terms using Metascape, color code reflecting cluster annotations.

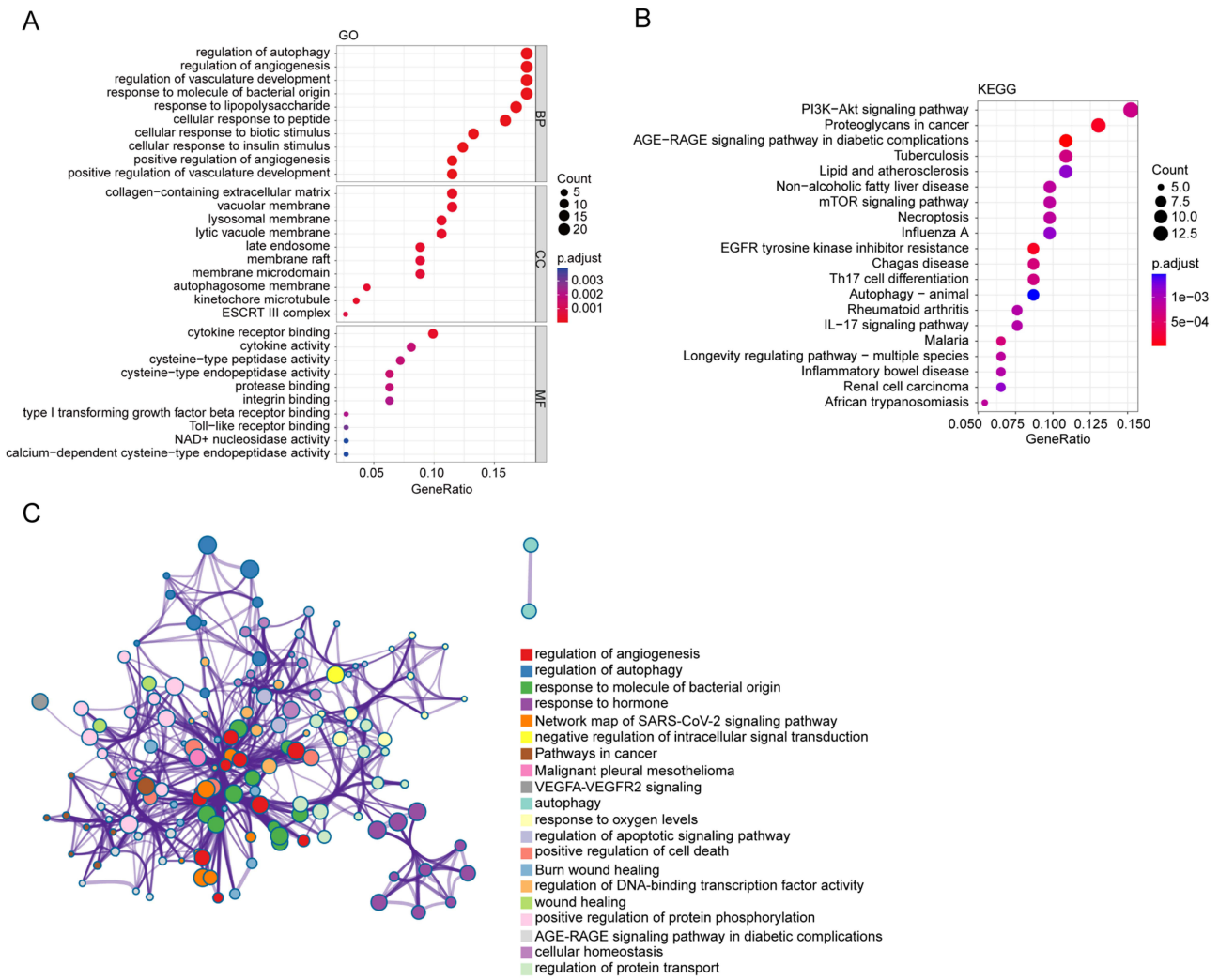


**Figure 3** Functional annotation of the autophagy-related DEGs. (**A**) GO enrichment analysis of the autophagy-related DEGs using R software. (**B**) KEGG enrichment analysis of the autophagy-related DEGs using R software. (**C**) The pathways network of the autophagy-related DEGs showing the intra-cluster and inter-cluster connections of enriched terms using Metascape, color code reflecting cluster annotations.

## Enrichment Analysis of the Hub Genes

To investigate the biological significance of these hub genes related to PANoptosis and autophagy, we performed functional and pathway enrichment analyses. The GO enrichment analysis revealed enrichment of cell chemotaxis, wound healing and positive regulation of MAPK cascade (Figure 5A). Furthermore, the KEGG enrichment analysis revealed that the hub genes were enriched in signaling pathways related to Cytokine−cytokine receptor interaction, the MAPK signaling pathway and the IL17 signaling pathway (Figure 5B). Additionally, as illustrated in Figures 5C and D, the results of the Metascape enrichment analysis displayed the functional annotations of this list of hub genes.

## The Hub Genes and Their Interactions

TFs are involved in gene transcription regulation. Furthermore, we investigated the interactions between these hub genes and TFs, shedding light on potential regulatory mechanisms. Our analysis revealed that 22 TFs coordinated with 10 PANoptosis-related hub genes, and 7 TFs coordinated with 4 autophagy-related hub genes, indicating significant cooperation between these hub genes and TFs (Figures 6A and B). Further, we analyzed the expression of these TFs in GSE206285 dataset and detected significant differences in these correlated TFs between UC patients and healthy controls (Figure 6C). This indicated that these TFs may influence the occurrence and development of UC.

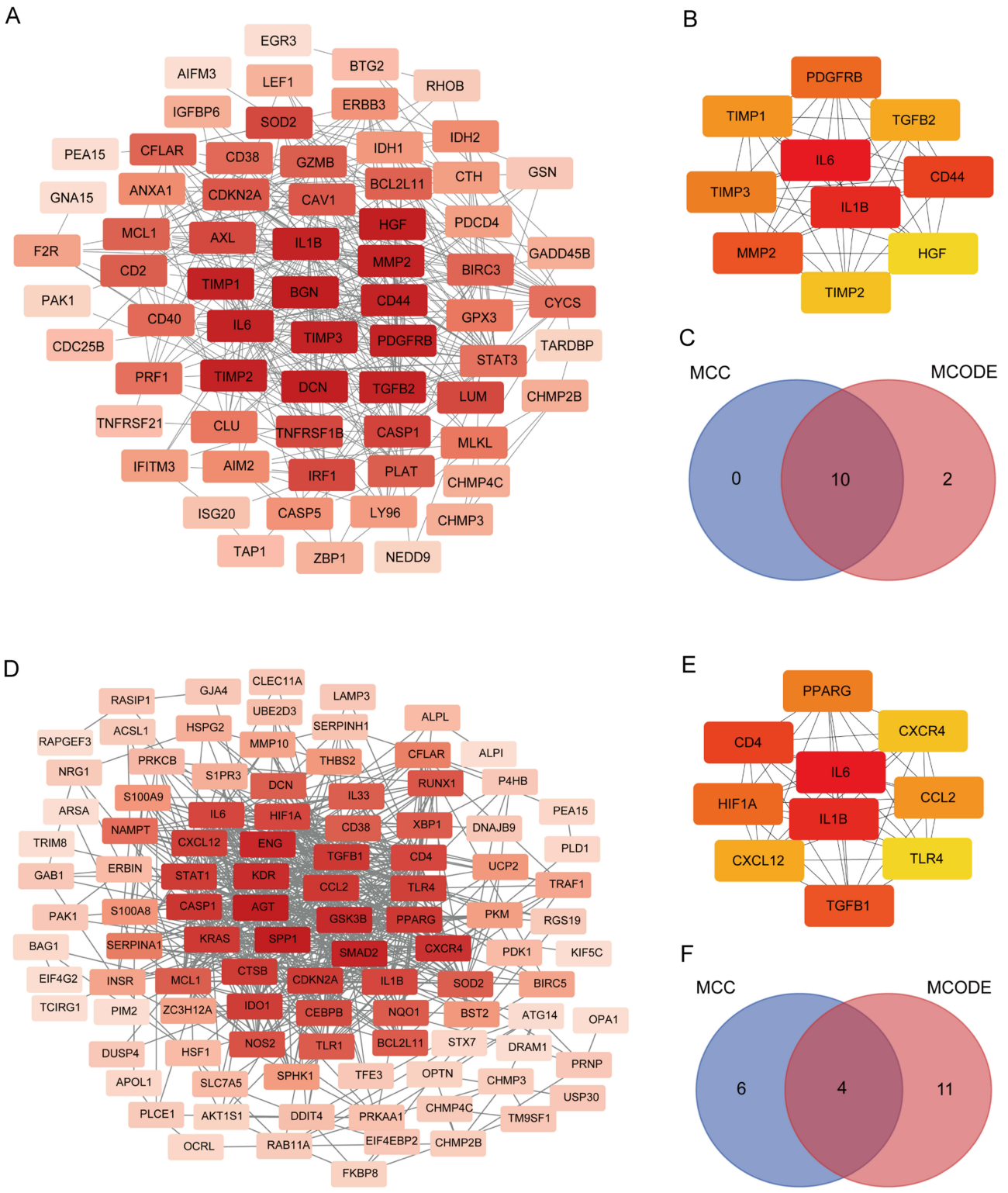


**Figure 4** The PPI network analysis of the PANoptosis-related DEGs and the autophagy-related DEGs. (**A**) The PPI network of the PANoptosis-related DEGs, the darker the color is, the more important the gene is. The top 12 PANoptosis-related DEGs, highlighted in the darkest color, were identified using MCODE. (**B**) The top 10 PANoptosis-related DEGs using MCC, the darker the color, the more critical the gene. (**C**) A Venn diagram of the intersection of the PANoptosis-related DEGs using MCC and MCODE analysis module. (**D**) The PPI network of the autophagy-related DEGs, the darker the color is, the more important the gene is. The top 15 autophagy-related DEGs, highlighted in the darkest color, were identified using MCODE. (**E**) The top 10 autophagy-related DEGs using MCC, the darker the color, the more critical the gene. (**F**) A Venn diagram of the intersection of the autophagy-related DEGs using MCC and MCODE analysis module.

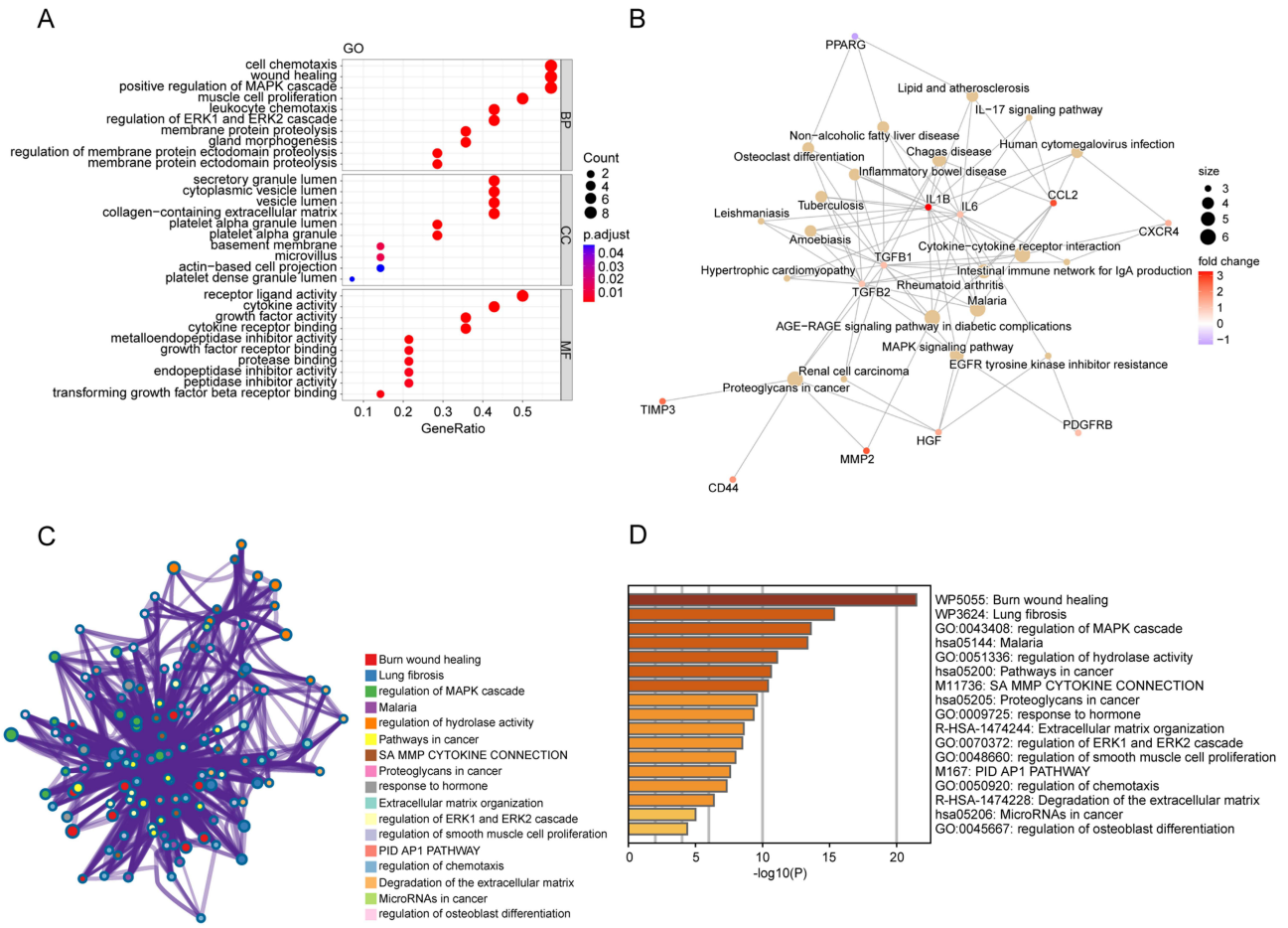


**Figure 5** Functional annotation of the PANoptosis- and autophagy-related hub genes. (**A**) GO enrichment analysis of the PANoptosis- and autophagy-related hub genes using R software. (**B**) KEGG enrichment pathway network of the PANoptosis- and autophagy-related hub genes using R software. (**C**) The pathways network of the hub genes using Metascape, color code reflecting cluster annotations. (**D**) The enrichment clusters analysis of the hub genes using Metascape.

We also predicted miRNA interactions and drug interactions for PANoptosis- and autophagy-related hub genes, as illustrated in Supplementary Figure 2 and 3. This analysis suggested that the drugs targeting these genes may hold potential for UC treatment. For example, sulfasalazine, which interacted with autophagy-related hub gene, PPARG, is mainly used for IBD, and can prevent the recurrence of UC.

## Immune Infiltration Analysis in UC

Dysregulated intestinal immune response plays a central role in the pathogenesis of UC. To explore the immune landscape of UC patients, the CIBERSORT algorithm was applied to evaluate the abundance of 22 immune cell subtypes in the GSE206285 dataset. Significant differences in immune-infiltrating cells were observed between the two groups. Compared to the normal group, UC patients demonstrated higher infiltration of plasma cells, activated memory $CD4^+$ T cells, M0 Macrophages, M1 Macrophages, activated dendritic cells, and neutrophils, while UC patients had significantly lower infiltration of memory B cells, resting memory $CD4^+$ T cells, and M2 macrophages (Figure 7A). In addition, as illustrated in Supplementary Figure 4, we conducted a correlation analysis among 22 categories of immune cells, demonstrating that most immunocytes were closely connected. Further analyses were conducted to shed light on the correlation between the hub genes and immune cells. We found that almost all PANoptosis-related hub genes were positively correlated with neutrophils, M0 macrophages, activated dendritic cells and activated memory $CD4^+$ T cells, while they were negatively correlated with resting memory $CD4^+$ T cells, M2 macrophages and Tregs regulatory T cells (Figure 7B). The autophagy-related hub genes, including CXCR4, CCL2, and TGFB1, showed positive correlations with

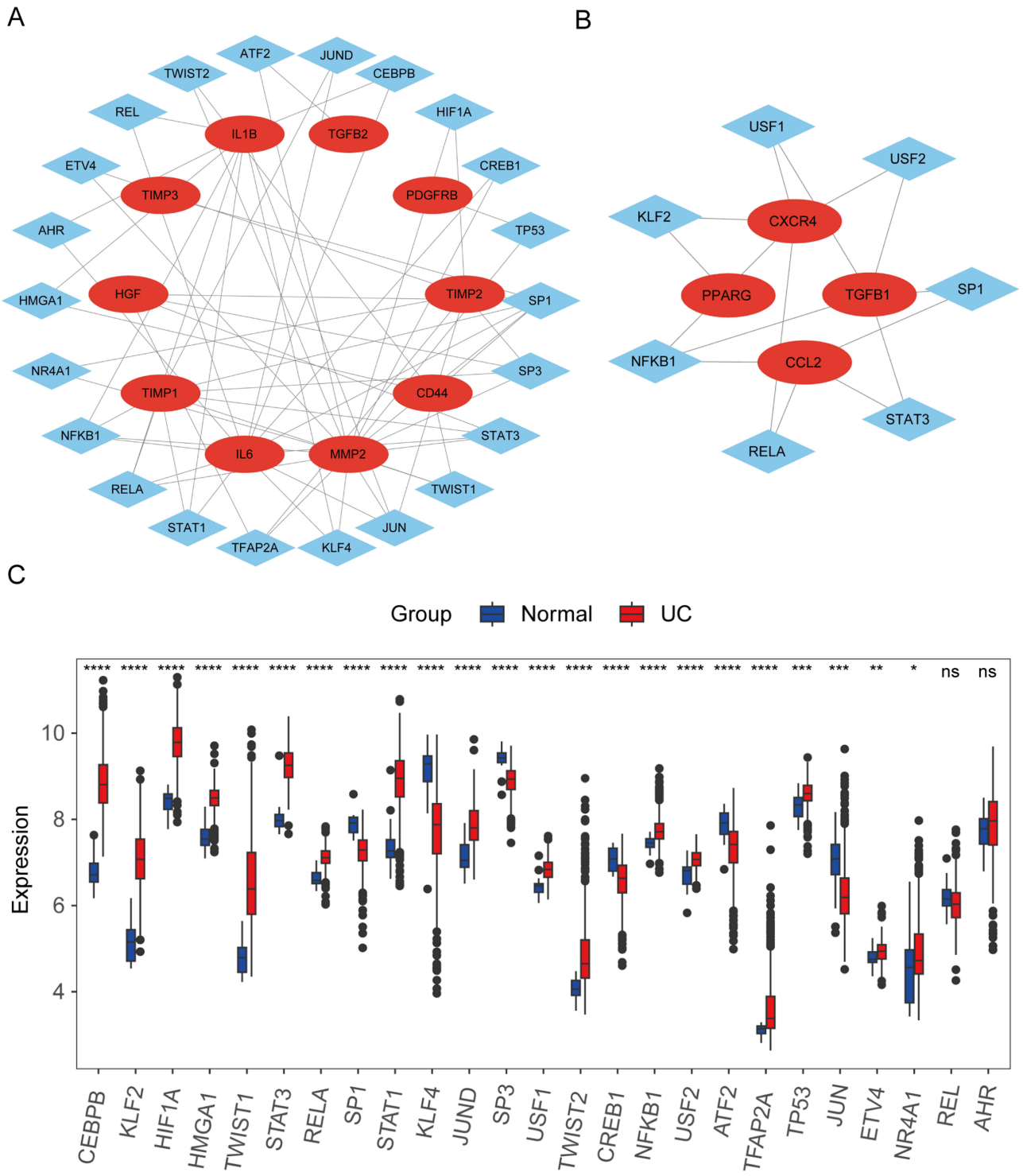


**Figure 6** Interactions between hub genes and TFs. (**A**) Prediction of TF genes and their interaction network with the PANoptosis-related hub genes. (**B**) Prediction of TF genes and their interaction network with the autophagy-related hub genes. (**C**) Expression differences of the 25 TF genes in the GSE206285 dataset sample. *p < 0.05; **p < 0.01; ***p < 0.001; ****p < 0.0001.

neutrophils, activated memory CD4$^+$ T cells, activated mast cells, M0 macrophages and activated dendritic cells, while they exhibited significant negative correlations with M2 macrophages, Tregs regulatory T cells, resting dendritic cells and resting mast cells. In contrast, PPARG showed quite the opposite pattern among these immune cells (Figure 7C). Based

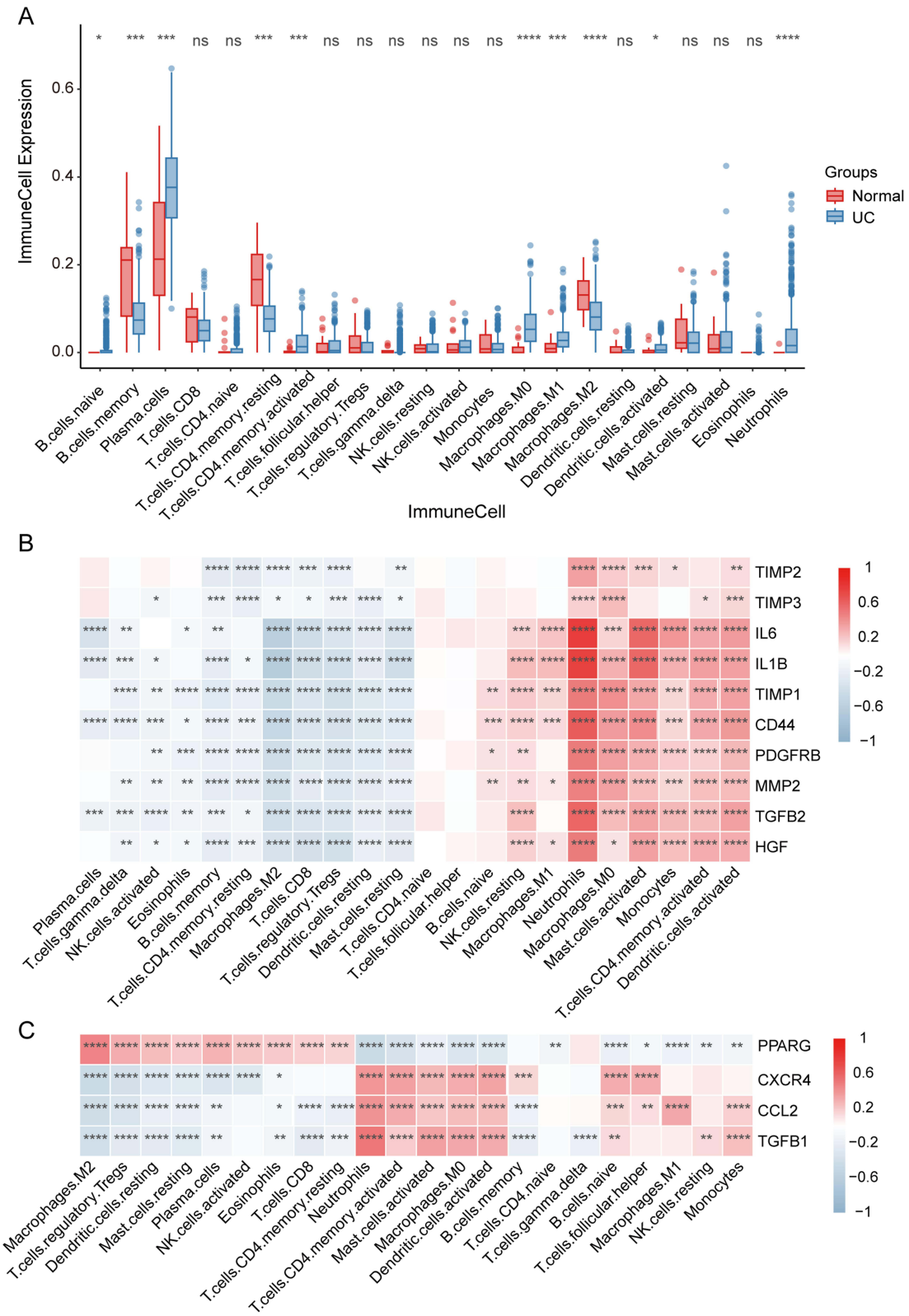


**Figure 7** The landscape of immunocyte infiltration. (**A**) Expression differences of 22 distinct immune infiltrating cells between UC and normal groups. (**B**) The correlation heatmap of the PANoptosis-related hub genes and immune infiltrating cells in UC. (**C**) The correlation heatmap of the autophagy-related hub genes and immune infiltrating cells in UC. *p < 0.05; **p < 0.01; ***p < 0.001; ****p < 0.0001.
**Abbreviation**: ns, no significance.

on these results, we could speculate that the PANoptosis- and autophagy-related hub genes may play a role in UC by regulating immunocytes.

## Single-Cell Sequencing Analysis of the Hub Genes

Subsequent single-cell sequencing data analysis revealed differential expression patterns of the hub genes across various cell compartments, providing insights into their roles in UC pathogenesis. UC-associated single-cell sequencing data were screened using Single Cell Portal, which identified 51 cell subsets in colon mucosa of 18 UC and 12 healthy individuals. Utilizing t-SNE method to annotate the cells within each sample into epithelial, immune and stromal compartments, and then clustering cells from multiple samples into distinct subtypes.[37] As shown in Figure 8A, epithelial t-SNE identified 15 cell subtypes, immune t-SNE identified 23 cell subtypes, and stromal t-SNE identified 13 cell subtypes. The results indicated that most hub genes were highly expressed in inflammatory fibroblasts (IAFs), except for PPARG and CXCR4. PPARG was mainly expressed in epithelial compartments, especially in immature enterocytes 2, enterocytes, and best4$^{+}$ enterocytes, while CXCR4 was predominantly expressed in immune compartments, particularly in ILCs, Follicular, and DC1 (Figure 8B). Numerous genes exhibit cell type specificity and function differently within distinct cell types. We found significant differences in the expression of these hub genes among these three cell compartments between UC patients and healthy controls. Moreover, their expression levels varied between inflamed and normal states in different cell types. For example, compared to the healthy population, the expression of TIMP1 and MMP2 was increased in the inflamed epithelial and stromal cells of UC patients but showed downregulation in the immune cells of UC patients (Figure 8C). These hub genes may operate within different cell subtypes implicated in the progression of UC.

## Construction of the ceRNA Network

To provide a comprehensive view of their regulatory interactions, we constructed ceRNA networks for both PANoptosis- and autophagy-related hub genes. The ceRNA network was established by employing miRNAs as intermediaries, where lncRNAs act as miRNA sponges through competitive binding with miRNAs, effectively sequestering miRNAs from the endogenous RNA. Utilizing miRTarBase, TarBase and TargetScan, we predicted 21 overlapping miRNAs of the PANoptosis-related hub genes, and a ceRNA network was developed, involving 10 PANoptosis-related hub genes, 21 miRNAs and 139 lncRNAs (Supplementary Figure 5). Similarly, we constructed a ceRNA network of the autophagy-related hub genes, involving 4 autophagy-related hub genes, 7 projected miRNAs and 60 lncRNAs (Supplementary Figure 6). Overall, these findings have significantly enriched our understanding of the regulatory expression of these hub genes.

## Identification of the Key Candidate Genes in UC via Machine Learning

To further identify the key candidate genes associated with UC pathogenesis, we compiled clinical characteristics data from UC patients. LASSO regression was employed to identify hub signature genes in UC. Ultimately, we identified five key genes as the most characteristic hub genes, including TIMP1, TIMP2, TIMP3, IL6, and CCL2 (Figure 9A). These five key candidate genes exhibited closely positively correlated with one another (Figure 9B). We subsequently generated ROC curves and computed the AUC for these key candidate genes to assess their diagnostic effectiveness. The results indicated that the diagnostic model, based on the five key genes, demonstrated high diagnostic performance in the GSE206285 dataset, with AUC values exceeding 0.7 for each of the five key genes (Figure 9C). We validated this model in two additional datasets, GSE16879 and GSE87466, both of which exhibited improved diagnostic efficacy. Among the five key genes, TIMP1 had the highest AUC value, which is significant (Figures 9D and E). Hence, the five key candidate genes may be involved in the occurrence of UC and exhibit excellent diagnostic value.

## External Verification of the Key Candidate Genes and the Clinical Significance

Subsequently, we verified the differential expression of these five key candidate genes using two additional datasets, GSE75214 and GSE114527. The results indicated that the identified key genes were expressed at higher levels in UC patients compared to healthy controls (Supplementary Figure 7). Furthermore, to determine whether the key candidate

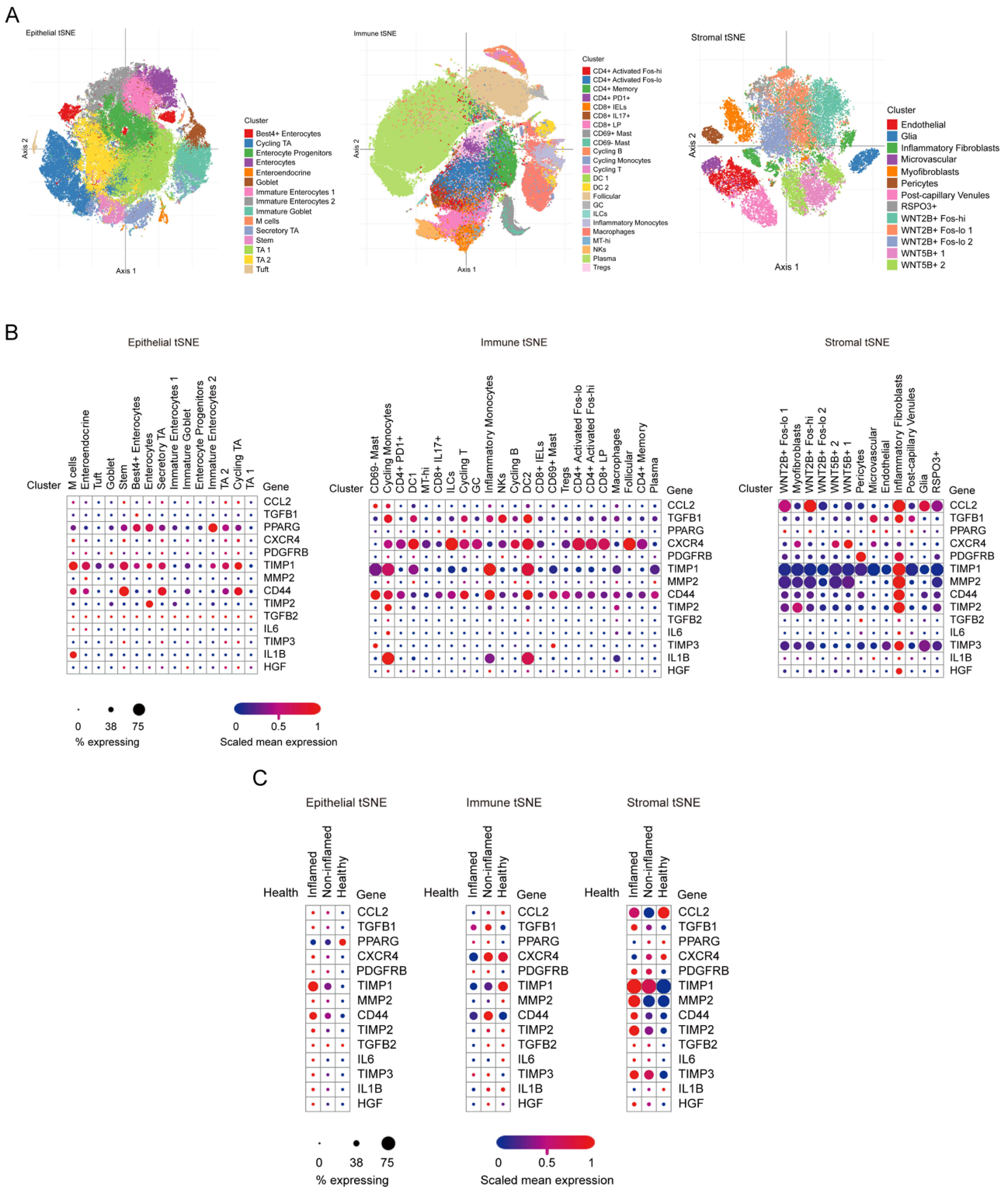


**Figure 8** The cell distribution and expression of the hub genes in UC. (**A**) The single-cell profiles partitioned into three compartments (epithelial, immune and stromal) including 51 subsets by clustering of colon biopsies from UC patients and healthy individuals. Shown is t-Stochastic Neighborhood Embedding (t-SNE) of cells colored by cell subset. (**B**) The cell subset distribution and expression of hub genes in three compartments. (**C**) The disease state (healthy, non-inflamed, or inflamed) distribution and expression of hub genes in three compartments.

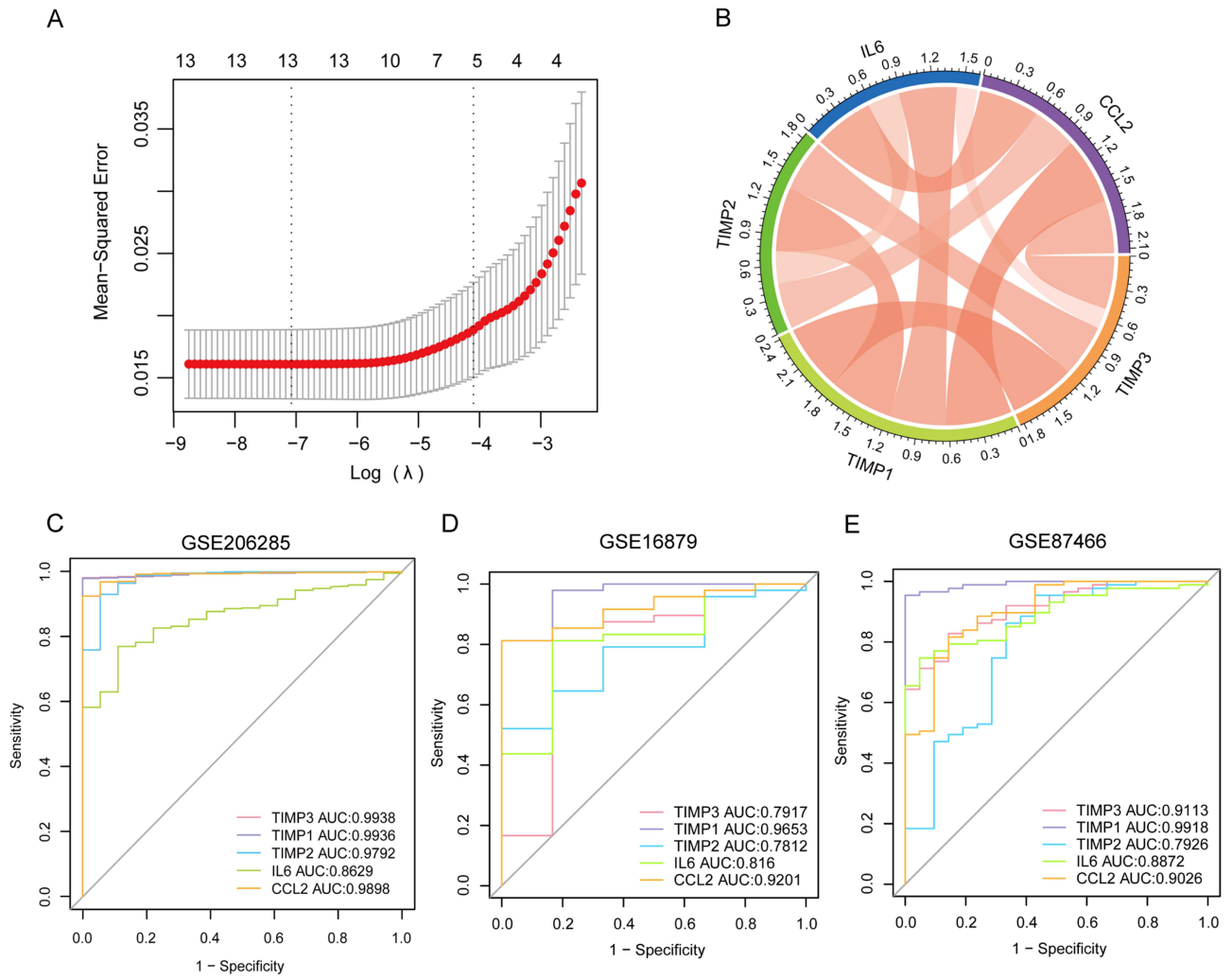


**Figure 9** Diagnostic model construction and identification of the key candidate genes. (**A**) LASSO regression in the identification of the key candidate genes. (**B**) Circle diagram displaying the correlation between the key candidate genes. ROC curves verifying the diagnostic performance of key candidate genes in (**C**) GSE206285, (**D**) GSE16879, (**E**) GSE87466 datasets.

genes were associated with clinical severity, we included new datasets GSE73661 and GSE92415 containing clinical disease activity data of UC patients to assess the expression of these genes across different disease severity levels of UC. We observed significant differences in the expression of these key candidate genes among UC patients with varying disease severity levels (Figures 10A and C). Meanwhile, we further analyzed the correlation between the expression of these genes and clinical scores. Importantly, we observed a positive correlation between the expression of these genes and UC-related clinical activity scores, with TIMP1 showing the strongest correlation and TIMP3 exhibiting weaker correlation (Figures 10B and D). These results indicated their involvement in the development of UC and their potential utility as disease severity biomarkers in UC patients.

## Validation of the Key Candidate Genes Using qRT-PCR

To complement the bioinformatics findings and confirm the involvement of the five key candidate genes in UC, we utilized qRT-PCR to validate their differential expression in colonic mucosal tissues of UC patients and UC mice model. The main clinical characteristics of the UC patients and healthy controls are summarized in Supplementary Table 3. In comparison to the healthy control group, patients with UC exhibited significant upregulation in the gene expression levels of TIMP1, TIMP3, IL6, and CCL2, with no significant difference observed in the expression levels of TIMP2 between the two groups (Figure 11A). Moreover, a DSS-induced acute colitis mouse model, simulating the clinical pathology of

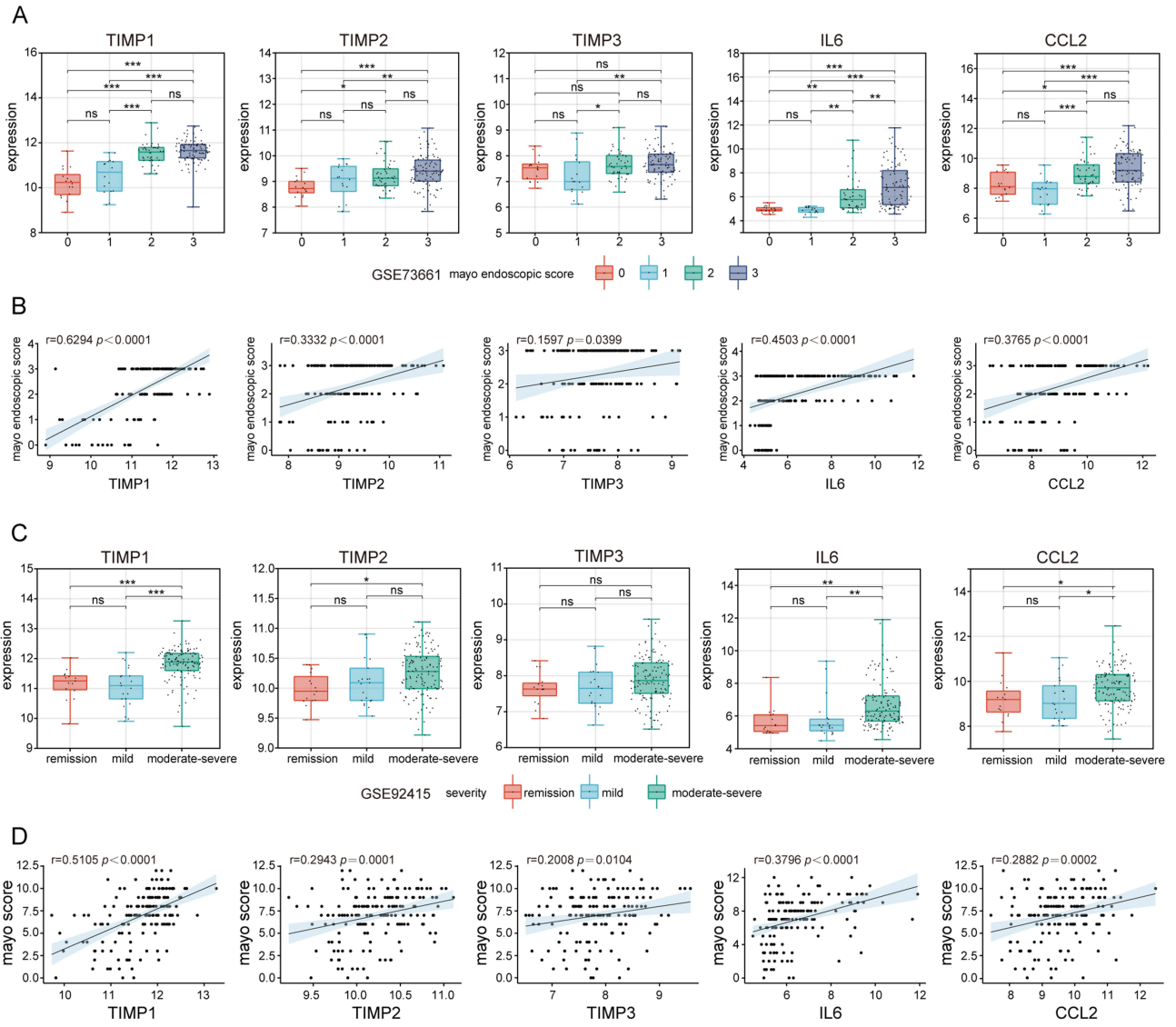


**Figure 10** Evaluation of the key candidate genes expression across UC severity levels and correlation with clinical scores. In GSE73661 dataset, TIMP1, TIMP2, TIMP3, IL6, and CCL2 levels varied with UC severity (**A**), and correlation analysis was performed between their expression and UC-related clinical scores (**B**). In GSE92415 dataset, TIMP1, TIMP2, TIMP3, IL6, and CCL2 levels differed across disease stages in UC (**C**), and correlation analysis was conducted between their expression and UC-related clinical scores (**D**). *p < 0.05; **p < 0.01; ***p < 0.001.
**Abbreviation**: ns, no significance.

UC, was effectively constructed. This was evidenced by H&E staining, which showed that DSS-treated mice exhibited epithelial erosion and inflammation in the colon (Figure 11B). qRT-PCR analysis revealed upregulated expression of the TIMP1, TIMP3, IL6, and CCL2 genes in colonic tissues of DSS-treated mice compared to the control group. The expression levels of TIMP2 did not differ significantly (Figure 11C).

## Discussion

Research on cell death mechanisms draws extensive attention, particularly focusing on programmed cell death (PCD),[43] which is essential for normal development and homeostasis maintenance. However, dysregulated cell death can trigger inflammation and modulate immune responses, thus necessitating strict regulation to prevent disease.[44] Currently, emerging concepts like PANoptosis,[6] Cuproptosis,[45] and Disulfidptosis[46] are being highlighted. While apoptosis, pyroptosis, necroptosis, and autophagy have been extensively investigated in UC,[47–49] recent research has also explored the involvement of ferroptosis and cuproptosis in this condition.[50,51] However, there is limited research on the regulatory

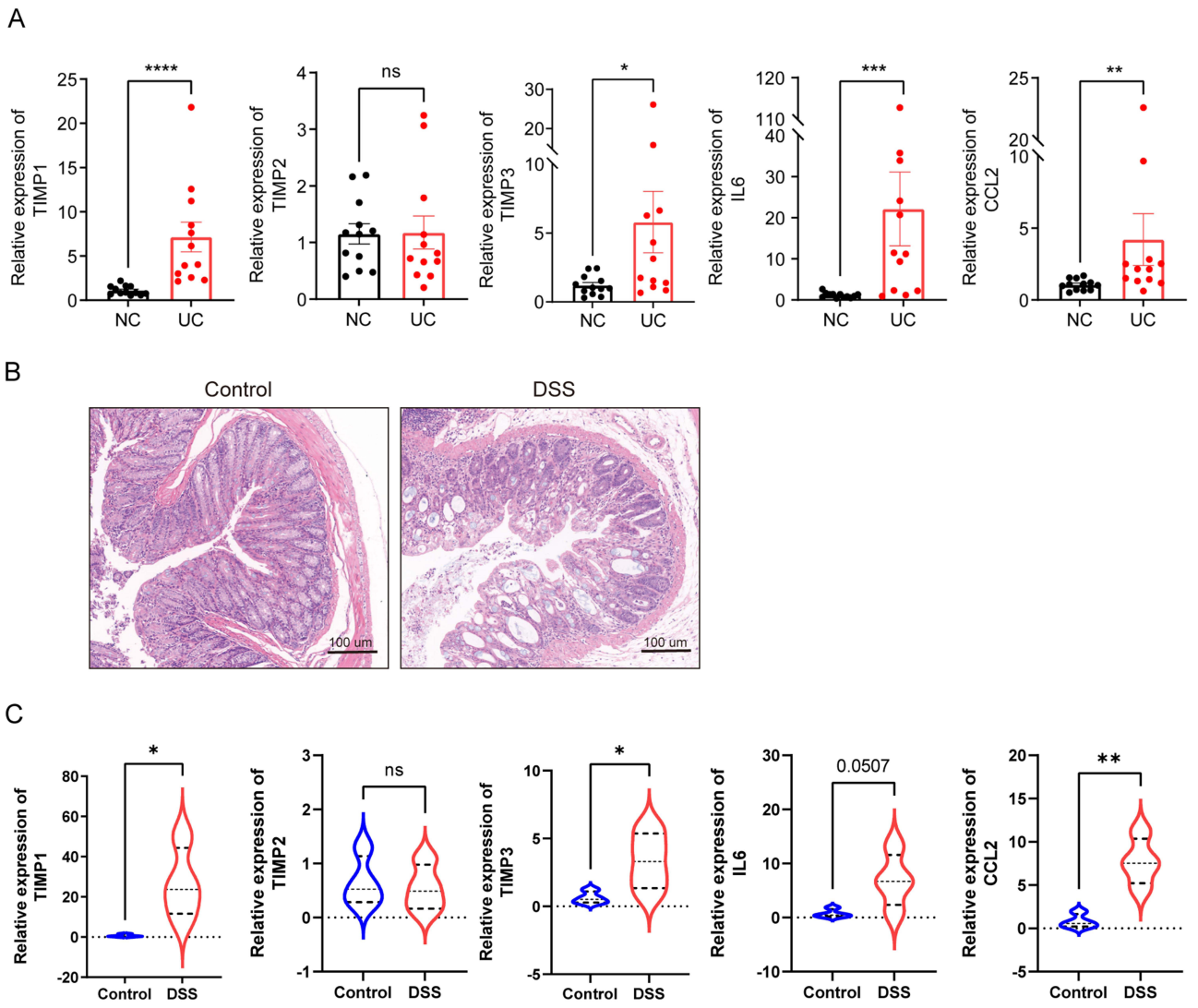


**Figure 11** Validation of the key candidate genes via qRT-PCR. (**A**) Relative mRNA expression levels of TIMP1, TIMP2, TIMP3, IL6, and CCL2 in colon mucosa of healthy controls (n = 12) and UC patients (n = 12). (**B**) Representative H&E staining of mouse distal colon sections collected from the water group and DSS group. (**C**) Relative mRNA expression levels of TIMP1, TIMP2, TIMP3, IL6, and CCL2 in the mouse colonic tissue of the water group (n=4) and DSS group (n=4). Mean ± SEM are plotted; *p < 0.05; **p < 0.01; ***p < 0.001; ****p < 0.0001.
**Abbreviation**: ns, no significance.

role of PANoptosis in UC. PANoptosis combines the main characteristics of pyroptosis, apoptosis, and necroptosis, while autophagy has been shown to coincide various forms of cell death.[52] Through bioinformatics and experimental verification, our study identified key genes related to PANoptosis and autophagy, potentially influencing immune dysregulation and wound healing in UC.

In this study, we obtained 71 PANoptosis- and 113 autophagy-related DEGs in GSE206285 dataset. Enrichment analyses revealed their involvement in wound healing, TNF signaling pathway and PI3K-Akt signaling pathway. The shared enriched pathways may unveil the underlying mechanisms behind the crosstalk between PANoptosis and autophagy pathways. Additionally, through PPI network analysis, we identified ten PANoptosis- and four autophagy-related hub genes involved in cell chemotaxis, wound healing and positive regulation of MAPK cascade. In UC, excessive neutrophil chemotaxis and activation serve as markers of poor outcomes and resistance to ustekinumab therapy.[22] Wound healing, particularly mucosal healing, is a crucial therapeutic endpoint and objective in UC management, correlating with improved long-term prognosis.[53–55] Moreover, the MAPK signaling pathway is closely linked to the pathogenesis of UC.[56] These results underlining the reliability of our enrichment analysis. Furthermore, focusing on

hub genes, we predicted key TFs associated with UC. Several TFs identified in our study play significant roles in inflammation, such as NFKB1, STAT1, STAT3.[57–59] Among them, CEBPB was found to be overexpressed in the mucosa of UC patients and potentially involved in the disease.[60–62] Our study provides the foundation for further investigations into the underlying roles of these TFs in UC.

Additionally, immune infiltration analysis revealed significantly altered immunocyte landscapes in UC patients, characterized by higher infiltration of plasma cells, activated memory CD4+ T cells, M1 Macrophages, activated dendritic cells (DCs) and neutrophils, along with decreased levels of memory B cells and M2 macrophages compared to healthy controls. Research has demonstrated that plasma cells play a pivotal role in UC-associated inflammatory infiltrates, and their expansion is associated with an increased risk of clinical relapse.[63,64] Restoring immune balance by inhibiting macrophage M1 polarization and promoting M2 polarization is a valuable therapeutic strategy for UC.[65] Neutrophil infiltration severity correlates with disease activity in UC and is incorporated into the scoring system for disease activity.[66] Correlation analysis between the hub genes and immunocytes revealed that most PANoptosis- and autophagy-related hub genes, except for PPARG, exhibited significant positive correlations with the infiltration of neutrophils, M0 macrophages, and activated dendritic cells. Conversely, they showed negative correlations with M2 macrophages. However, PPARG displayed contrasting behavior. These findings suggest a potential involvement of hub genes in UC onset through modulation of immune cell activity, warranting further mechanistic exploration.

The emerging single-cell sequencing technology can assess gene expression in single cells and potentially provide cell-level insights into the disease.[67] Our analysis of single-cell sequencing data highlighted elevated expression of hub genes in inflammatory fibroblasts, with the exception of PPARG and CXCR4. The raw report findings suggested that an inflammation-associated fibroblast (IAFs) subset is unique to the UC colon and enriched for expression of many genes associated with colitis, fibrosis, and cancer.[37] In IBDs and other inflammatory diseases, fibroblasts are recognized as major contributors and regulators of inflammation.[68–70] Research on fibroblasts in IBDs pointed that IAFs were associated with resistance to anti-TNF therapy by compensating during TNF blockade, thus contributing to therapy resistance.[37,71] While previous research into cell death in UC primarily focused on intestinal epithelial cells, which trigger inflammation by compromising barrier integrity, there has been limited exploration of the role of fibroblast death in UC. We conceived an audacious idea that manipulating the death pathways of inflammatory fibroblasts may offer novel therapeutic avenues for UC treatment. Our results have identified molecular targets; however, further research is warranted to elucidate these mechanisms fully. Our identification of molecular targets associated with IAFs provides valuable insights for the development of targeted therapies aimed at modulating the inflammatory microenvironment in UC.

Moreover, we also identified five key candidate genes: TIMP1, TIMP2, TIMP3, IL6, and CCL2, closely linked to UC pathogenesis through LASSO regression analysis of clinical characteristics data. The diagnostic efficacy of the five key genes assessed by ROC curves in the three datasets showed good predictive value and stability. Tissue Inhibitor of Metalloproteinases (TIMP) family, including TIMP1, TIMP2, TIMP3, and TIMP4, are renowned for inhibiting Matrix Metalloproteinases (MMPs), crucial regulators in inflammation and wound healing in IBD.[72] However, TIMPs also exhibit diverse cellular functions beyond MMP inhibition, such as involvement in PCD[73] and inflammation regulation. Recent findings have highlighted TIMP1 as an emerging cytokine in inflammation.[74] High TIMP1 levels have been shown to activate neutrophils and directly trigger formation of neutrophil extracellular traps (NETs),[75] a neutrophil-specific PCD pattern known to be involved in many autoimmune inflammatory diseases.[76] We speculate on TIMP1's potential role in mediating PANoptosis and contributing to its proinflammatory effects in UC. TIMP2 has been demonstrated to mediate inflammation and apoptosis by regulating the NF-κB pathway and has been implicated in NLRP3-mediated pyroptosis.[77,78] A prospective pilot study indicated that reduced serum TIMP2 levels during anti-TNF-α antibody treatment were associated with short- and long-term disease remission, suggesting its potential as a prognostic indicator in IBD.[79] TIMP3 inhibits TACE (TNF-α converting enzyme), a protease involved in generating soluble TNF-α, thus regulating TNF-α and inflammation.[80] However, TACE inhibition could amplified TNF-α-mediated hyperpermeability, suggesting a potential autocrine effect of TIMP3 on epithelial barrier disruption.[81] Previous study reported that interaction between CCL2 and IL6 in the tumor microenvironment inhibits caspase-8 cleavage and subsequent activation of the caspase-cascade, inducing autophagy and M2-type macrophage polarization, thus promoting tumorigenesis.[82] Understanding their reciprocal induction and effects on caspase cascades and autophagy in the inflammatory microenvironment requires further investigation. Targeting these cytokines in combination

may represent a promising strategy in therapeutics of UC. Additionally, the positive correlation between the five key genes and the clinical severity of UC patients implies their potential utility as disease severity biomarkers in UC patients.

Finally, we validated the expression of the five key candidate genes in colon mucosa of both UC patients and UC mice model using qRT-PCR. The results indicated a significant upregulation of TIMP1, TIMP3, IL6, and CCL2 mRNA levels in UC compared to normal controls. However, TIMP2 mRNA levels showed no significant difference, which aligns with the findings of a previous study.[83] The study measured mRNA expression by quantitative PCR as well and observed that TIMP1 mRNA was significantly increased in inflamed, and especially ulcerated, colon mucosa from IBD patients whereas TIMP2 mRNA expression remained unchanged.[83] This discrepancy may be attributed to the fact that we both utilized whole colon homogenate tissues to assess gene expression levels, instead of analyzing specific cell subtypes, as genes can display distinct expression patterns and functions across different cell types. Additionally, protein-level validation is also necessary. Hence, the aforementioned findings indicated the need for further investigation at the single-cell level to elucidate cell-specific expression patterns and functions in UC progression.

Nonetheless, our study has a few limitations. First, the conclusions are primarily derived from bioinformatics analyses, necessitating further experimental validation. Second, the influence of treatments on gene expression in validation datasets GSE16879 warrants consideration. Third, despite demonstrating promising diagnostic efficacy and stability within UC, further research is indeed needed to thoroughly evaluate specificity and applicability of the identified markers in the diagnostic context. Finally, the sample size included to verify is relatively small. We aspire to include a larger quantity of UC samples, preferably at the single-cell level, to delve deeper into the potential molecular mechanisms of PANoptosis and autophagy in UC.

## Conclusion

In this study, we identified key genes associated with PANoptosis and autophagy, including TIMP1, TIMP2, TIMP3, IL6, and CCL2, potentially influencing immune dysregulation and wound healing in UC. Our findings underscore the significance of PANoptosis and autophagy in UC pathogenesis, particularly through their regulation of immune cells and inflammatory fibroblasts. Further validation through fundamental experiments at the single-cell level is needed to corroborate our findings regarding PANoptosis and autophagy. Our study provides insights into the potential clinical applications of targeting PANoptosis and autophagy pathways for improved treatment of UC.

## Data Sharing Statement

The online repositories and detailed datasets information supporting the conclusions of this article are included within the Materials and Methods section of the manuscript. Further reasonable inquiries can be directed to the corresponding author.

## Ethics Approval and Consent to Participate

This research received approval from the Medical Ethics Committee, Zhongnan Hospital of Wuhan University (Scientific Ethical Approval No.2022011K). The procedures employed in this study adhere to the tenets of the Declaration of Helsinki. All participants informed and consent. Animal experiments were approved by the Animal Ethics committee of Zhongnan Hospital, Wuhan University. All procedures followed the Chinese guidelines for the welfare of the laboratory animals (GB/T 35892-2018).

## Acknowledgments

We thank all the subjects who participated in this study. We thank Dr Zhao Ding of Zhongnan Hospital, Wuhan University, for assistance in specimen collection. This paper has been uploaded to Research Square as a preprint: https://doi.org/10.21203/rs.3.rs-3482634/v1.

## Author Contributions

All authors made a significant contribution to the work reported, whether that is in the conception, study design, execution, acquisition of data, analysis and interpretation, or in all these areas; took part in drafting, revising or critically

reviewing the article; gave final approval of the version to be published; have agreed on the journal to which the article has been submitted; and agree to be accountable for all aspects of the work.

## Funding

This work was supported by the Key Project of Medical Science and Technology Innovation Platform Construction Support of Zhongnan Hospital of Wuhan University (PTXM2022007).

## Disclosure

The authors declare no competing interests in this work.

## References

1. Gros B, Kaplan GG. Ulcerative Colitis in Adults: a Review. *JAMA*. 2023;330(10):951–965.
2. Shao X, Sun S, Zhou Y, et al. Bacteroides fragilis restricts colitis-associated cancer via negative regulation of the NLRP3 axis. *Cancer Lett*. 2021;523:170–181.
3. Graham DB, Xavier RJ. Pathway paradigms revealed from the genetics of inflammatory bowel disease. *Nature*. 2020;578(7796):527–539.
4. Xavier RJ, Podolsky DK. Unravelling the pathogenesis of inflammatory bowel disease. *Nature*. 2007;448(7152):427–434.
5. Patankar JV, Becker C. Cell death in the gut epithelium and implications for chronic inflammation. *Nat Rev Gastroenterol Hepatol*. 2020;17(9):543–556.
6. Samir P, Malireddi RKS, Kanneganti TD. The PANoptosome: a Deadly Protein Complex Driving Pyroptosis, Apoptosis, and Necroptosis (PANoptosis). *Front Cell Infect Microbiol*. 2020;10:238.
7. Zheng M, Kanneganti TD. The regulation of the ZBP1-NLRP3 inflammasome and its implications in pyroptosis, apoptosis, and necroptosis (PANoptosis). *Immunol Rev*. 2020;297(1):26–38.
8. Lee S, Karki R, Wang Y, et al. AIM2 forms a complex with pyrin and ZBP1 to drive PANoptosis and host defence. *Nature*. 2021;597(7876):415–419.
9. Pandian N, Kanneganti TD. PANoptosis: a Unique Innate Immune Inflammatory Cell Death Modality. *J Immunol*. 2022;209(9):1625–1633.
10. Christgen S, Tweedell RE, Kanneganti TD. Programming inflammatory cell death for therapy. *Pharmacol Ther*. 2022;232:108010.
11. Zhu P, Ke ZR, Chen JX, et al. Advances in mechanism and regulation of PANoptosis: prospects in disease treatment. *Front Immunol*. 2023;14:1120034.
12. Arab HH, Al-Shorbagy MY, Saad MA. Activation of autophagy and suppression of apoptosis by dapagliflozin attenuates experimental inflammatory bowel disease in rats: targeting AMPK/mTOR, HMGB1/RAGE and Nrf2/HO-1 pathways. *Chem. Biol. Interact.* 2021;335:109368.
13. Lv Q, Xing Y, Liu J, et al. Lonicerin targets EZH2 to alleviate ulcerative colitis by autophagy-mediated NLRP3 inflammasome inactivation. *Acta pharmaceutica Sinica B*. 2021;11(9):2880–2899.
14. Wang R, Li H, Wu J, et al. Gut stem cell necroptosis by genome instability triggers bowel inflammation. *Nature*. 2020;580(7803):386–390.
15. Foerster EG, Mukherjee T, Cabral-Fernandes L, et al. How autophagy controls the intestinal epithelial barrier. *Autophagy*. 2022;18(1):86–103.
16. Takahama M, Akira S, Saitoh T. Autophagy limits activation of the inflammasomes. *Immunol Rev*. 2018;281(1):62–73.
17. Larabi A, Barnich N, Nguyen HTT. New insights into the interplay between autophagy, gut microbiota and inflammatory responses in IBD. *Autophagy*. 2020;16(1):38–51.
18. Don Wai Luu L, Kaakoush NO, Castaño-Rodríguez N. The role of ATG16L2 in autophagy and disease. *Autophagy*. 2022;18(11):2537–2546.
19. Nguyen HT, Lapaquette P, Bringer MA, Darfeuille-Michaud A. Autophagy and Crohn's disease. *J Innate Immunity*. 2013;5(5):434–443.
20. Sazonovs A, Stevens CR, Venkataraman GR, et al. Large-scale sequencing identifies multiple genes and rare variants associated with Crohn's disease susceptibility. *Nature Genet*. 2022;54(9):1275–1283.
21. Cabrera S, Fernández AF, Mariño G, et al. ATG4B/autophagin-1 regulates intestinal homeostasis and protects mice from experimental colitis. *Autophagy*. 2013;9(8):1188–1200.
22. Pavlidis P, Tsakmaki A, Pantazi E, et al. Interleukin-22 regulates neutrophil recruitment in ulcerative colitis and is associated with resistance to ustekinumab therapy. *Nat Commun*. 2022;13(1):5820.
23. Li K, Strauss R, Ouahed J, et al. Molecular Comparison of Adult and Pediatric Ulcerative Colitis Indicates Broad Similarity of Molecular Pathways in Disease Tissue. *J Pediatr Gastroenterol Nutr*. 2018;67(1):45–52.
24. Arijs I, De Hertogh G, Lemaire K, et al. Mucosal gene expression of antimicrobial peptides in inflammatory bowel disease before and after first infliximab treatment. *PLoS One*. 2009;4(11):e7984.
25. Lorén V, Garcia-Jaraquemada A, Naves JE, et al. ANP32E, a Protein Involved in Steroid-Refractoriness in Ulcerative Colitis, Identified by a Systems Biology Approach. *J Crohn's Colitis*. 2019;13(3):351–361.
26. Arijs I, De Hertogh G, Lemmens B, et al. Effect of vedolizumab (anti-α4β7-integrin) therapy on histological healing and mucosal gene expression in patients with UC. *Gut*. 2018;67(1):43–52.
27. Vancamelbeke M, Vanuytsel T, Farré R, et al. Genetic and Transcriptomic Bases of Intestinal Epithelial Barrier Dysfunction in Inflammatory Bowel Disease. *Inflammatory bowel dis*. 2017;23(10):1718–1729.
28. Sandborn WJ, Feagan BG, Marano C, et al. Subcutaneous golimumab induces clinical response and remission in patients with moderate-to-severe ulcerative colitis. *Gastroenterology*. 2014;146(1):85–95.
29. Shi X, Gao X, Liu W, et al. Construction of the panoptosis-related gene model and characterization of tumor microenvironment infiltration in hepatocellular carcinoma. *Oncol Res*. 2023;31(4):569–590.
30. Wang NN, Dong J, Zhang L, et al. HAMdb: a database of human autophagy modulators with specific pathway and disease information. *J Cheminf*. 2018;10(1):34.

31. Zhou Y, Zhou B, Pache L, et al. Metascape provides a biologist-oriented resource for the analysis of systems-level datasets. *Nat Commun*. 2019;10(1):1523.
32. Szklarczyk D, Kirsch R, Koutrouli M, et al. The STRING database in 2023: protein-protein association networks and functional enrichment analyses for any sequenced genome of interest. *Nucleic Acids Res*. 2023;51(D1):D638–d646.
33. Han H, Cho JW, Lee S, et al. TRRUST v2: an expanded reference database of human and mouse transcriptional regulatory interactions. *Nucleic Acids Res*. 2018;46(D1):D380–d386.
34. Huang HY, Lin YC, Cui S, et al. miRTarBase update 2022: an informative resource for experimentally validated miRNA-target interactions. *Nucleic Acids Res*. 2022;50(D1):D222–d230.
35. Wishart DS, Feunang YD, Guo AC, et al. DrugBank 5.0: a major update to the DrugBank database for 2018. *Nucleic Acids Res*. 2018;46(D1):D1074–d1082.
36. Newman AM, Liu CL, Green MR, et al. Robust enumeration of cell subsets from tissue expression profiles. *Nature Methods*. 2015;12(5):453–457.
37. Smillie CS, Biton M, Ordovas-Montanes J, et al. Intra- and Inter-cellular Rewiring of the Human Colon during Ulcerative Colitis. *Cell*. 2019;178(3):714–730.e722.
38. Karagkouni D, Paraskevopoulou MD, Chatzopoulos S, et al. DIANA-TarBase v8: a decade-long collection of experimentally supported miRNA-gene interactions. *Nucleic Acids Res*. 2018;46(D1):D239–d245.
39. McGeary SE, Lin KS, Shi CY, et al. The biochemical basis of microRNA targeting efficacy. *Science (New York, NY)*. 2019;366(6472):582.
40. Li JH, Liu S, Zhou H, Qu LH, Yang JH. starBase v2.0: decoding miRNA-ceRNA, miRNA-ncRNA and protein-RNA interaction networks from large-scale CLIP-Seq data. *Nucleic Acids Res*. 2014;42(Database issue):D92–97.
41. Yang C, Delcher C, Shenkman E, Ranka S. Machine learning approaches for predicting high cost high need patient expenditures in health care. *Biomed. Eng. Online*. 2018;17(Suppl 1):131.
42. Spandidos A, Wang X, Wang H, Seed B. PrimerBank: a resource of human and mouse PCR primer pairs for gene expression detection and quantification. *Nucleic Acids Res*. 2010;38(Database issue):D792–799.
43. Griffioen AW, Nowak-Sliwinska P. Programmed cell death lives. *Int j Programmed Cell Death*. 2022;27(9–10):619–621.
44. Kayagaki N, Webster JD, Newton K. Control of Cell Death in Health and Disease. *Ann Rev Pathol*. 2023.
45. Tsvetkov P, Coy S, Petrova B, et al. Copper induces cell death by targeting lipoylated TCA cycle proteins. *Science (New York, NY)*. 2022;375(6586):1254–1261.
46. Liu X, Nie L, Zhang Y, et al. Actin cytoskeleton vulnerability to disulfide stress mediates disulfidptosis. *Nat Cell Biol*. 2023;25(3):404–414.
47. Liu Q, Du P, Zhu Y, et al. Thioredoxin reductase 3 suppression promotes colitis and carcinogenesis via activating pyroptosis and necrosis. *Cell Mol Life Sci*. 2022;79(2):106.
48. Su W, Chen Y, Cao P, et al. Fusobacterium nucleatum Promotes the Development of Ulcerative Colitis by Inducing the Autophagic Cell Death of Intestinal Epithelial. *Front Cell Infect Microbiol*. 2020;10:594806.
49. Wan Y, Yang L, Jiang S, Qian D, Duan J. Excessive Apoptosis in Ulcerative Colitis: crosstalk Between Apoptosis, ROS, ER Stress, and Intestinal Homeostasis. *Inflammatory bowel dis*. 2022;28(4):639–648.
50. Yang C, Wang W, Li S, et al. Identification of cuproptosis hub genes contributing to the immune microenvironment in ulcerative colitis using bioinformatic analysis and experimental verification. *Front Immunol*. 2023;14:1113385.
51. Yokote A, Imazu N, Umeno J, et al. Ferroptosis in the colon epithelial cells as a therapeutic target for ulcerative colitis. *J Gastroenterol*. 2023;58(9):868–882.
52. Levine B, Kroemer G. Autophagy in the pathogenesis of disease. *Cell*. 2008;132(1):27–42.
53. Cholapranee A, Hazlewood GS, Kaplan GG, Peyrin-Biroulet L, Ananthakrishnan AN. Systematic review with meta-analysis: comparative efficacy of biologics for induction and maintenance of mucosal healing in Crohn's disease and ulcerative colitis controlled trials. *Aliment. Pharmacol. Ther.* 2017;45(10):1291–1302.
54. Peyrin-Biroulet L, Sandborn W, Sands BE, et al. Selecting Therapeutic Targets in Inflammatory Bowel Disease (STRIDE): determining Therapeutic Goals for Treat-to-Target. *Am J Gastroenterol*. 2015;110(9):1324–1338.
55. Shah SC, Colombel JF, Sands BE, Narula N. Mucosal Healing Is Associated With Improved Long-term Outcomes of Patients With Ulcerative Colitis: a Systematic Review and Meta-analysis. *Clin gastroenterol hepatol*. 2016;14(9):1245–1255.e1248.
56. Zhou M, Xu W, Wang J, et al. Boosting mTOR-dependent autophagy via upstream TLR4-MyD88-MAPK signalling and downstream NF-κB pathway quenches intestinal inflammation and oxidative stress injury. *EBioMedicine*. 2018;35:345–360.
57. Bharadwaj U, Kasembeli MM, Robinson P, Tweardy DJ. Targeting Janus Kinases and Signal Transducer and Activator of Transcription 3 to Treat Inflammation, Fibrosis, and Cancer: rationale, Progress, and Caution. *Pharmacol Rev*. 2020;72(2):486–526.
58. Cartwright T, Perkins ND, Lw C. NFKB1: a suppressor of inflammation, ageing and cancer. *FEBS J*. 2016;283(10):1812–1822.
59. Yu YL, Chen M, Zhu H, et al. STAT1 epigenetically regulates LCP2 and TNFAIP2 by recruiting EP300 to contribute to the pathogenesis of inflammatory bowel disease. *Clin epigenetics*. 2021;13(1):127.
60. Boyd M, Thodberg M, Vitezic M, et al. Characterization of the enhancer and promoter landscape of inflammatory bowel disease from human colon biopsies. *Nat Commun*. 2018;9(1):1661.
61. Nowak JK, Adams AT, Kalla R, et al. Characterisation of the Circulating Transcriptomic Landscape in Inflammatory Bowel Disease Provides Evidence for Dysregulation of Multiple Transcription Factors Including NFE2, SPI1, CEBPB, and IRF2. *J Crohn's Colitis*. 2022;16(8):1255–1268.
62. Ufer M, Häsler R, Jacobs G, et al. Decreased sigmoidal ABCB1 (P-glycoprotein) expression in ulcerative colitis is associated with disease activity. *Pharmacogenomics*. 2009;10(12):1941–1953.
63. Bessissow T, Lemmens B, Ferrante M, et al. Prognostic value of serologic and histologic markers on clinical relapse in ulcerative colitis patients with mucosal healing. *Am J Gastroenterol*. 2012;107(11):1684–1692.
64. El-Zimaity H, Shaffer SR, Riddell RH, Pai RK, Bernstein CN. Beyond Neutrophils for Predicting Relapse and Remission in Ulcerative Colitis. *J Crohn's Colitis*. 2023;17(5):767–776.
65. Wu MM, Wang QM, Huang BY, et al. Dioscin ameliorates murine ulcerative colitis by regulating macrophage polarization. *Pharmacol Res*. 2021;172:105796.
66. Bressenot A, Salleron J, Bastien C, et al. Comparing histological activity indexes in UC. *Gut*. 2015;64(9):1412–1418.

67. Liu Z, Li H, Dang Q, et al. Integrative insights and clinical applications of single-cell sequencing in cancer immunotherapy. *Cell Mol Life Sci*. 2022;79(11):577.
68. Kinchen J, Chen HH, Parikh K, et al. Structural Remodeling of the Human Colonic Mesenchyme in Inflammatory Bowel Disease. *Cell*. 2018;175 (2):372–386.e317.
69. Nguyen HN, Noss EH, Mizoguchi F, et al. Autocrine Loop Involving IL-6 Family Member LIF, LIF Receptor, and STAT4 Drives Sustained Fibroblast Production of Inflammatory Mediators. *Immunity*. 2017;46(2):220–232.
70. Wei K, Nguyen HN, Brenner MB. Fibroblast pathology in inflammatory diseases. *J Clin Invest*. 2021;131(20).
71. Martin JC, Chang C, Boschetti G, et al. Single-Cell Analysis of Crohn's Disease Lesions Identifies a Pathogenic Cellular Module Associated with Resistance to Anti-TNF Therapy. *Cell*. 2019;178(6):1493–1508.e1420.
72. Kobayashi K, Arimura Y, Goto A, et al. Therapeutic implications of the specific inhibition of causative matrix metalloproteinases in experimental colitis induced by dextran sulphate sodium. *J Pathol*. 2006;209(3):376–383.
73. Mannello F, Gazzanelli G. Tissue inhibitors of metalloproteinases and programmed cell death: conundrums, controversies and potential implications. *Int j Programmed Cell Death*. 2001;6(6):479–482.
74. Schoeps B, Frädrich J, Krüger A. Cut loose TIMP-1: an emerging cytokine in inflammation. *Trends Cell Biol*. 2023;33(5):413–426.
75. Schoeps B, Eckfeld C, Prokopchuk O, et al. TIMP1 Triggers Neutrophil Extracellular Trap Formation in Pancreatic Cancer. *Cancer Res*. 2021;81 (13):3568–3579.
76. Mutua V, Gershwin LJ. A Review of Neutrophil Extracellular Traps (NETs) in Disease: potential Anti-NETs Therapeutics. *Clinical Reviews in Allergy & Immunology*. 2021;61(2):194–211.
77. Li YM, Zhang J, Su LJ, Kellum JA, Peng ZY. Downregulation of TIMP2 attenuates sepsis-induced AKI through the NF-κb pathway. *Biochim. Biophys. Acta, Mol. Basis Dis*. 2019;1865(3):558–569.
78. Shi S, Zhang C, Liu J. TIMP2 facilitates CIRI through activating NLRP3-mediated pyroptosis. *Aging*. 2023;15(9):3635–3643.
79. Carbone F, Bodini G, Brunacci M, et al. Reduction in TIMP-2 serum levels predicts remission of inflammatory bowel diseases. *Eur. J. Clin. Invest*. 2018;48(10):e13002.
80. Mohammed FF, Smookler DS, Taylor SE, et al. Abnormal TNF activity in Timp3-/- mice leads to chronic hepatic inflammation and failure of liver regeneration. *Nature Genet*. 2004;36(9):969–977.
81. Fréour T, Jarry A, Bach-Ngohou K, et al. TACE inhibition amplifies TNF-alpha-mediated colonic epithelial barrier disruption. *IntJ Mol Med*. 2009;23(1):41–48.
82. Roca H, Varsos ZS, Sud S, et al. CCL2 and interleukin-6 promote survival of human CD11b+ peripheral blood mononuclear cells and induce M2-type macrophage polarization. *J Biol Chem*. 2009;284(49):34342–34354.
83. von Lampe B, Barthel B, Coupland SE, Riecken EO, Rosewicz S. Differential expression of matrix metalloproteinases and their tissue inhibitors in colon mucosa of patients with inflammatory bowel disease. *Gut*. 2000;47(1):63–73.